Eur Biophys J (1999) 28: 119–132

ARTICLE

José García de la Torre · Stephen E. Harding
Beatriz Carrasco

Calculation of NMR relaxation, covolume, and scattering-related properties of bead models using the SOLPRO computer program

Received: 25 May 1998 / Revised version: 30 July 1998 / Accepted: 30 July 1998

Abstract The hydrodynamic properties of macromolecules and bioparticles, represented by bead models, can be calculated using methods implemented in the computer routine HYDRO. Recently, a new computer routine, SOLPRO, has been presented for the calculation of various SOLution PROperties. These include (1) time-dependent electro-optic and spectroscopic properties related to rotational diffusion, (2) non-dynamic properties like scattering curves, and (3) dimensionless quantities that combine two or more solution properties in a form which depends on the shape of the macromolecule but not on its size. In the present work we describe the inclusion of more of those types of properties in a new version of SOLPRO. Particularly, we describe the calculation of relaxation rates in nuclear magnetic resonance (NMR). For dipolar coupling, given the direction of the dipole the program calculates values of the spectral density, from which the NMR relaxation times can be obtained. We also consider scattering-related properties, namely the distribution of distances for the bead model, which is directly related to the angular dependence of scattered intensity, and the particle's longest distance. We have devised and programmed a procedure to calculate the covolume of the bead model, related to the second virial coefficient and, in general, to the concentration dependence of solution properties. Various shape-dependent dimensionless quantities involving the covolume are calculated. In this paper we also discuss some aspects, namely bead overlapping and hydration, that are not explicitely included in SOLPRO, but should be considered by the user.

J. García de la Torre (✉) · B. Carrasco
Departamento de Química Física, Universidad de Murcia,
E-30071 Murcia, Spain
e-mail: jgt@fcu.um.es

S. E. Harding
Department of Applied Biochemistry & Food Science,
University of Nottingham, Sutton Bonington, LE12 5RD, UK

Key words SOLPRO computer program · Hydrodynamics · NMR relaxation · Macromolecules · Molecular covolume · Immunoglobulin IgG3

Introduction

The hydrodynamic properties of rigid macromolecules and bioparticles can be conveniently calculated by representing the molecule as bead models (Bloomfield et al. 1967; García de la Torre and Bloomfield 1977) whose hydrodynamics is described by theoretical and computational procedures (García de la Torre and Bloomfield 1981; García de la Torre 1989) which are now implemented in the public-domain HYDRO computer program (García de la Torre et al. 1994). Recently, the present authors have developed further this methodology, presenting another public-domain program, SOLPRO, for calculating additional SOLution PROperties (García de la Torre et al. 1997). In a typical calculation, HYDRO is called first to obtain the basic hydrodynamic properties, namely the translational diffusion coefficient, sedimentation coefficient, intrinsic viscosity, rotational coefficients, and relaxation times. Next, the subroutine SOLPRO can be called to calculate more advanced dynamic properties, particularly time-dependent birefringence and fluorescence anisotropy, or non-dynamic properties such as angular dependence of radiation scattering. Another utility of SOLPRO is the calculation of quantities that combine hydrodynamic and non-hydrodynamic solution properties in dimensionless forms which have the important feature of depending on the shape of the macromolecule, but not on its size (Harding 1995).

In the present work, we report the inclusion in SOLPRO of new solution properties which extend the applicability of bead modeling using HYDRO+SOLPRO. In experimental work, solution properties are obtained for various solute concentrations, and the values extrapolated to infinite dilution are the primary results to be used in structural analysis. However, the concentration dependence (usually, the slope in a property versus concentration plot) also

contains information on the size and shape of the macromolecular solute. The concentration dependences can be expressed in terms of the quantity called molecular covolume (Ogston and Winzor 1975; Harding and Johnson 1985a), which has been now included in SOLPRO.

It is known that rotational quantities (rotational diffusion coefficients and relaxation times) are among the properties most sensitive to the detailed size and shape of the macromolecule. These quantities are experimentally obtained in a somehow indirect, rather involved manner from instrumental techniques that monitor the rotational dynamics. In the previous version of SOLPRO we extended the HYDRO calculation of rotational diffusion and relaxation times to predict the results of two such techniques: transient electric birefringence and fluorescence anisotropy decay. Another technique which is gaining popularity recently is NMR relaxation spectroscopy, which is being used to gain insight into the detailed shape and backbone dynamics of proteins (see, for instance, Clore et al. 1990, Barbato et al. 1992, Tjandra et al. 1995) and nucleic acids (see, for instance, Birchall and Lane 1990; Eimer et al. 1990; Nuutero et al. 1994). In the new SOLPRO subroutine we have programmed the calculation of the correlation and spectral density functions from which the NMR quantities, such relaxation rates and nuclear Overhauser effect (NOE) enhancement, can be predicted.

As commented above, in the former version of SOLPRO we included the calculation of a non-hydrodynamic property, the angular dependence of radiation scattered by the macromolecule in solution, i.e., the form or structure factor. For the same bead models used for hydrodynamics a Debye-formula calculation of the form factor, including the influence of the elements (beads) was presented. In the field of X-ray scattering there exists a common practice of transforming the experimental angular dependence into a distribution of distances between points in the particle, expressing as a final result the distance distribution function (Glatter and Kratky 1982). In the new SOLPRO we have implemented analytical formulas that give the distribution of distances between points in an array of spheres and some characteristic particle distances and lengths.

Dynamic NMR

For dipolar chemical shift anisotropy and quadrupolar relaxation mechanisms, relaxation rate constants are linear combinations of values of the spectral density function, $J(\omega)$, particularized by some specific characteristic values of the frequency ω.

A simple but frequent example is the dipolar interaction between a proton (^{1}H) and a different nucleus X (such as X = ^{13}C or ^{15}N) (Palmer et al. 1996). The NMR relaxation times, T_1 and T_2, respectively, and the NOE enhancement are calculated from $J(\omega)$ (Abragam 1961) as linear combinations of the values $J(\omega_H-\omega_X)$, $J(\omega_H)$, $J(\omega_X)$, $J(\omega_H+\omega_X)$, and $J(0)$, where ω_X is the Larmor frequency of the X nucleus (Evans 1995). For the full expressions of T_1, T_2, and NOE, see, for instance, Clore et al. (1990). The spectral density function is related to the rotational dynamics of the macromolecule by means of the fundamental relationship

$$J(\omega) = \int_0^\infty \left\langle P_2\left[\boldsymbol{\mu}(0)\cdot\boldsymbol{\mu}(t)\right]\right\rangle \cos(\omega t)\,\mathrm{d}t \tag{1}$$

$\boldsymbol{\mu}$ is a vector defining the orientation of the axis of the relaxation interaction, i.e., a vector along the X-H vector in the case of dipolar interaction given here as an example. $\boldsymbol{\mu}(0)$ and $\boldsymbol{\mu}(t)$ are the orientations of the X-H vector at some initial time (0) and after some time (t) has elapsed. The scalar product $\boldsymbol{\mu}(0)\cdot\boldsymbol{\mu}(t) = \cos\theta(t)$ where $\theta(t)$ is the angle subtended by those two orientations, and $P_2(c) \equiv (3c^2-1)/2$ is the second-Legendre polynomial of $c = \cos(\theta(t))$.

Thus, the problem of calculating NMR relaxation quantities reduces to the determination of the correlation function

$$P_2(t) = \langle P_2(\boldsymbol{\mu}(0)\cdot\boldsymbol{\mu}(t))\rangle \tag{2}$$

where $\boldsymbol{\mu}$ is a specific unitary vector within the particle.

When the particle is a rigid body (in the absence of any internal motion), as is assumed in the context of HYDRO/SOLPRO, the evaluation of the correlation function implicit in Eq. (2), for a vector $\boldsymbol{\mu}$ attached to a rigid particle of arbitrary shape, is a general problem that appears in a variety of situations. This problem was solved in the fundamental work of Favro (1960), and applied to NMR relaxation by various workers (Woessner 1962; Huntress 1968). If μ_k (k = 1, 2, 3 or x, y, z) are the components of vector $\boldsymbol{\mu}$ in a Cartesian system of coordinates whose axes along the directions of the rotational diffusion tensor, $\boldsymbol{D}_r$, then the correlation function is a sum of up to five exponentials:

$$P_2(t) = \sum_{l=1}^{5} a_l \exp(-t/\tau_l) \tag{3}$$

The five rotational relaxation times are the same as for other rotational properties (Favro 1960; García de la Torre and Bloomfield 1981; García de la Torre et al. 1997):

$$\tau_1 = (6D - 2\Delta)^{-1} \tag{4}$$

$$\tau_2 = (3(D + D_1))^{-1} \tag{5}$$

$$\tau_3 = (3(D + D_2))^{-1} \tag{6}$$

$$\tau_4 = (3(D + D_3))^{-1} \tag{7}$$

$$\tau_5 = (6D + 2\Delta)^{-1} \tag{8}$$

where D_1, D_2, D_3 are the eigenvalues of $\boldsymbol{D}_r$ in an ascending order, and

$$D = (1/3)\,\mathrm{Tr}\,\boldsymbol{D}_r \tag{9}$$

$$\Delta = (D_1^2 + D_2^2 + D_3^2 - D_1D_2 - D_1D_3 - D_2D_3)^{1/2} \tag{10}$$

Tr indicates the trace of a matrix, i.e., the sum of its diagonal components.

The amplitudes, a_l, in Eq. (3) are given by

$$a_1 = \frac{3}{4}(F' + G') \tag{11}$$

$$a_2 = 3\,\mu_2^2\,\mu_3^2 \tag{12}$$

$$a_3 = 3\,\mu_1^2\,\mu_3^2 \tag{13}$$

$$a_4 = 3\,\mu_1^2\,\mu_2^2 \tag{14}$$

$$a_5 = \frac{3}{4}(F' - G') \tag{15}$$

where

$$F' = -\frac{1}{3} + \sum_{k=1}^{3} \mu_k^4 \tag{16}$$

and

$$G' = \frac{1}{\Delta}\left(-D + \sum_{k=1}^{3} D_k\left[\mu_k^4 + 2\,\mu_m^2\,\mu_n^2\right]\right) \tag{17}$$

where m and n are the two other indices different from k. We use the notations F' and G' in Eqs. (11)–(17) to distinguish them from the related quantities F and G used in the calculation of fluorescence anisotropy decay.

The correlation function $P_2(t)$ decays to zero from $P_2(0) = 1$ for $t = 0$. Thus, the five coefficients obey the condition

$$\sum_{l=1}^{5} a_l = 1 \tag{18}$$

Mean and initial relaxation times, τ_{mean} and τ_{ini}, can be defined and calculated as described elsewhere (García de la Torre et al. 1997). In particular, the mean relaxation time is called the correlation time, τ_c (see below), in NMR literature:

$$\tau_{\mathrm{mean}} \equiv \tau_c = \int_0^\infty P_2(t)\,\mathrm{d}t = \sum_{l=1}^{5} a_l\,\tau_l \tag{19}$$

Now, going back to the NMR spectral density function, it turns out that, if $P_2(t)$ is a sum of exponentials, then for each component we have

$$\int_0^\infty \exp(t/\tau_l)\cos(\omega t)\,\mathrm{d}t = \frac{(1/\tau_l)}{\omega^2 + (1/\tau_l)^2} \tag{20}$$

so that, finally:

$$J(\omega) = \sum_{l=1}^{5} \frac{a_l\,\tau_l}{1 + \tau_l^2\,\omega^2} \tag{21}$$

Note that, as a consequence of the normalization of $P_2(t)$, it turns out from Eq. (18) that the zero frequency value of the spectral density function is

$$J(0) = \tau_{\mathrm{mean}} \tag{22}$$

The new version of SOLPRO calculates values of the $J(\omega)$ function. It accepts input data for the components of the unitary vector (μ_x, μ_y, μ_z) in the user's chosen particle-fixed system of coordinates. Internally, the $\boldsymbol{\mu}$ vector is transformed to the main axes of the rotational diffusion. Previously the rotational relaxation times τ_l and the amplitudes a_l are obtained, which allows the calculation of τ_c, as well as τ_{ini} and τ_{mean}. It is also possible to calculate, optionally, a table of $P_2(t)$ for a user-given range of times. Finally, $J(\omega)$ is evaluated for a set of ω values (combination of Larmor frequencies) specified by the user.

In order to avoid the complexity of the hydrodynamics of asymmetric particles (mostly, when software pieces like HYDRO and SOLPRO were not available), it has been a common practice in NMR relaxation to represent the particle by simplified models. For the sake of completeness we mention them in the present description. One of them is the axially symmetric rotor, with only two distinct rotational coefficients, $D_r^\perp$ and $D_r^\parallel$. For this case, only three components enter in $P_2(t)$ and in $J(\omega)$:

$$C(t) = a_1' \exp(-t/\tau_1') + a_2' \exp(-t/\tau_2') + a_3' \exp(-t/\tau_3') \tag{23}$$

$$J(\omega) = \frac{a_1'\,\tau_1'}{1 + \tau_1'^2\omega^2} + \frac{a_2'\,\tau_2'}{1 + \tau_2'^2\omega^2} + \frac{a_3'\,\tau_3'}{1 + \tau_3'^2\omega^2} \tag{24}$$

where $\tau_1' = (6\,D_r^\perp)^{-1}$, $\tau_2' = (D_r^\parallel + 5\,D_r^\perp)^{-1}$, $\tau_3' = (4\,D_r^\parallel + 2\,D_r^\perp)^{-1}$ and $a_1' = (3\cos^2\alpha - 1)/2$, $a_2' = 3\sin^2\alpha\cos^2\alpha$, $a_3' = (3\sin^4\alpha)/4$ (Woessner 1962; Huntress 1968; Barbato et al. 1992). Of course, Eqs. (23) and (24) are exactly valid for axially symmetric particles such as revolution ellipsoids and rods. Indeed, SOLPRO does not treat specially this case since the general equations are applicable without any problem. One just notices that two pairs of relaxation times coincide; for example (although necessarily in this order), we may obtain $\tau_2 = \tau_3 = \tau_2'$ and $\tau_4 = \tau_5 = \tau_3'$, with $a_2' = a_2' + a_3'$ and $a_3' = a_4' + a_5'$. Finally, a most common assumption in the interpretation of NMR relaxation has been to treat the particle as an isotropic rotor, either because the particle was in fact approximately spherical, or just as a simplifying assumption. For a spherical particle, $P_2(t)$ is a single exponential:

$$P_2(t) = \exp(-t/\tau_c) \tag{25}$$

where τ_c is the (single) rotational correlation relaxation time, and

$$J(\omega) = \tau_c/(1 + \tau_c^2\,\omega^2) \tag{26}$$

If Eq. (25) is considered just as an approximation, then it follows from Eq. (19) that $\tau_c = \tau_{\mathrm{mean}}$, accepting the fitting criterion that the area under $P_2(t)$ must be the same. Thus, the mean relaxation time reported by SOLPRO can be used to analyze experimental results elaborated in the isotropic-rotor hypothesis and presented as τ_c.

As described in our previous paper (García de la Torre et al. 1997), the first version of SOLPRO included the calculation of compound, dimensionless quantities that combine two or more solution properties in a form that depends on the shape but not on the size of particles. Some of these

quantities, or shape functions, that combine a rotational relaxation time with other properties, are:

$$\frac{\tau_k}{\tau_0} = \frac{kT}{\eta_0 V}\,\tau_k \tag{27}$$

$$\Psi_k \equiv \left(\frac{4\pi\,\eta_0}{3\,kT}\right)^{1/3} \frac{M_r(1-\bar{\upsilon}\,\rho_0)}{6\pi\,\eta_0\,N_A\,s}\left(\frac{1}{\tau_k}\right)^{1/3} = \left(\frac{\tau_0}{\tau_k}\right)^{1/3} P \tag{28}$$

$$\Lambda_k \equiv \frac{\eta_0[\eta]\,M_r}{N_A\,kT\,\tau_k} = \left[\frac{\tau_0}{\tau_k}\right]\nu \tag{29}$$

where η_0 and ρ_0 are the viscosity and density of the solvent, respectively, M_r is the molecular weight of the solute, $\bar{\upsilon}$ is the specific partial volume of the solute, $[\eta]$ is the intrinsic viscosity of the solution, s is the sedimentation coefficient, and N_A the Avogadro number. In Eqs. (27)–(29), τ_k can be any of the five main rotational relaxation times (k = 1,…,5). These are independent of the technique (birefringence, fluorescence polarization anisotropy, or NMR relaxation) used to monitor rotational diffusion. Also, τ_k in Eqs. (27)–(29) represents the mean, or the initial, or harmonic mean relaxation times. These are dependent on the technique, and therefore the NMR values, calculated in the new version of SOLPRO, will differ from those from other techniques.

Scattering properties

The angular variation of the intensity of radiation scattered by macromolecules in solution depends sensitively on the size and shape of the particle. As is well known, the radius of gyration of the macromolecule, R_g, which is a useful measure of macromolecular size, can be extracted from the low-angle (Zimm or Guinier) region of the scattering diagram. The full angular dependence over a wide angular region is expressed in terms of the so-called form factor $P(h)$, with $h = (4\pi/\lambda)\sin(\theta/2)$ where θ is the scattering angle and λ is the wavelength of the incident radiation in the solution. The $P(h)$ function depends remarkably on the shape of the particle.

For a bead model, composed of spherical elements, R_g and $P(h)$ are calculated by HYDRO and SOLPRO, respectively. By the way, we note that the first version of SOLPRO contained a programming error that was kindly reported by Dr. J. Gapinski (University of Poznan, Poland). The example of the $P(h)$ calculation in Fig. 5a, b of García de la Torre et al. (1997) was affected by that error, which has been corrected in the newer version of SOLPRO.

Now, we have included in SOLPRO the calculation of other scattering-related properties, namely the distance distribution and the longest chord, for models composed of spherical beads. Typical results for the scattering-related properties for the IgG3 bead model that we are using as example are shown in Figs. 4 and 5 (see later). The distribution of distances in Fig. 4 is obtained according to the procedure described below, and the scattering curves in Fig. 5a, b are calculated as described in our previous paper (García de la Torre et al. 1997). We are not aware of experimental data for this protein which could be used to test the results in Figs. 4 and 5, which are merely intended to illustrate a typical outcome from SOLPRO (and, by the way, to correct the above-mentioned error which affected two figures in our previous paper). Particularly, results for wide-angle scattering beyond the first or second minimum may be meaningless when h exceeds largely the reciprocal of the spatial resolution length of the bead model.

Distribution of distances

The angular dependence of the intensity of scattered radiation depends on the shape of the particles, which determines how the mass of the particle is spatially distributed. The scattering phenomenon is due to the interferences of the rays emitted by every pair of points within the particle. As a consequence, the normalized angular dependence of intensity (i.e. the "form factor" of the particle), $P(h)$, can be written in terms of the distribution of the distances, $p(r)$, between every two pairs of points within the macromolecule:

$$P(h) = \int_0^\infty p(r)\,\frac{\sin(h\,r)}{h\,r}\,\mathrm{d}r \tag{30}$$

and $p(r)$ is expressed as a Fourier transform:

$$p(r) = \frac{1}{2\,\pi^2}\int_0^\infty (h\,r)\,P(h)\sin(h\,r)\,\mathrm{d}h \tag{31}$$

with the normalization condition

$$\int_0^\infty p(r)\,\mathrm{d}r = 1 \tag{32}$$

In practice, the integrals over distance in Eqs. (30)–(32) can be extended up to an upper limit $r = L$, where L is the longest distance (also named longest chord) between points within the particle. This has the obvious property that $p(r) = 0$ for $r > L$. The distance distribution $p(r)$ can be obtained from the experimentally determined angular dependence of X-ray scattering intensities (Glatter and Kratky 1982).

The prediction of the distance distribution function for a rigid particle of arbitrary shape can be done only numerically. A finite (but necessary large) number, N_e, of scattering elements are placed within the particle. This can be programmed by superposition of a regular lattice (for instance, a simple cubic one) on the particle, taking into account all the points that fall within the particle. All the distances between the N_e^2 pairs of points are calculated, and a histogram of the distribution of these distances gives $p(r)$. If u is the separation between lattice points (i.e., the resolution of the model), the number of points is proportional to u^{-3} and the number of pairs and therefore the computing time grows as u^{-6}. For instance, increasing the resolution by a factor of 2 would increase the central processing

unit (CPU) time by a factor of 64. Then the determination of $p(r)$ with high resolution by this numerical procedure can be extremely time-consuming.

Fortunately, for the specific case of a bead model, i.e., when the particle is a rigid array of spheres, the above procedure can be avoided since $p(r)$ can be calculated from analytical expressions. Let $P_{11}(r; a)$ be the distribution of distances between points of a sphere of radius a. Also, let $P_{12}(r; a_1; a_2, d_{12})$ be the distribution of distances from points of a sphere of radius a_1 to points of a sphere of radius a_2, with center-to-center distance d_{12}. Then, for an array of N spheres, $p(r)$ can be expressed as a combination of P_{11} and P_{12}:

$$p(r) = \sum_{i=1}^{N} f_i^2 P_{11}(r; a_i) + 2 \sum_{i\neq}^{N} \sum_{j}^{N} f_i\ f_j\ P_{12}(r; a_1; a_2; d_{12}) \quad (33)$$

In Eq. (33) we have assumed the same uniform density (electron density for X-ray scattering) for all the beads, and f_i is the volume fraction of the bead: $f_i = V_i/\sum V_i = a_i/\sum a_i^3$.

In a standard monograph, the intra-sphere distribution P_{11} has been given as attributed to Porod (Glatter and Kratky 1982):

$$P_{11}(r) = \frac{3}{16\, a^6}\, r^2 (r - 2\, a)^2 (r + 4\, a) \quad (34)$$

but the inter-sphere distribution was not presented, so that we had to derive it. It turns out that the functional form of P_{12} depends on the range of r:

- If $d_{12} - a_1 - a_2 < r < d_{12} + a_1 - a_2$:

$$P_{12}(r) = \frac{3\, r}{160\, d_{12}\, a_1^3\, a_2^3} (a_1 + a_2 + q)^3 \quad (35)$$
$$(-4\, a_1^2 + 12\, a_1\, a_2 - 4\, a_2^2 - 3\, a_1\, q - 3\, a_2\, q + q^2)$$

- If $d_{12} + a_1 - a_2 < r < d_{12} - a_1 + a_2$:

$$P_{12}(r) = \frac{3\, r}{20\, d_{12}\, a_1^3\, a_2^3} (a_1)^3 (-a_1^2 + 5\, a_2^2 - 5\, q^2) \quad (36)$$

- If $d_{12} - a_1 + a_2 < r < d_{12} + a_1 + a_2$:

$$P_{12}(r) = \frac{3\, r}{160\, d_{12}\, a_1^3\, a_2^3} (a_1 + a_2 - q)^3 \quad (37)$$
$$(-4\, a_1^2 + 12\, a_1\, a_2 - 4\, a_2^2 + 3\, a_1\, q + 3\, a_2\, q + q^2)$$

where $q = r - d_{12}$.

Maximum dimension and moments of the distance distribution

As commented above, an important characteristic dimension of a rigid particle is the longest distance, or longest chord, defined as the maximum distance between any pair of points within the particle with $p(r) = 0$ for $r > L$. For a bead model, L can be calculated trivially:

$$L = r_{ij} + \sigma_i + \sigma_j \quad (38)$$

where (i, j) is the pair of beads for which the center-to-center distance, r_{ij}, is a maximum.

Although the longest chord can be defined and calculated rather trivially, the most important parameter related to the distance distribution is the square of the radius of gyration, R_g^2, which actually can be obtained from the second moment of the distribution:

$$R_g^2 = \frac{1}{2} \int_0^L r^2 p(r)\, dr \quad (39)$$

However, R_g^2 is more often determined from the low-angle behavior of the form factor. The term $\sin(h\, r)/(h\, r)$ in Eq. (30) can be expressed as a Taylor expansion in even powers, $(h\, r)^{2i}$. This leads to

$$P(h) = \sum_{i=0}^{\infty} \frac{(-1)^i\, 2\, R_{2i}\, h^{2i}}{(2\, i + 1)!} \quad (40)$$

where

$$R_{2i} = \frac{1}{2} \int_0^L r^{2i} p(r)\, dr \quad (41)$$

and $R_g^2 \equiv R_2$ ($2i = 2$). At very low angle, terms with $2i = 4, 6, \ldots$, can be neglected and $P(h)$ depends only on the second moment. Common expressions of the very-low-angle ($h \ll R_g^{-1}$) behavior, employed in analysis of experimental data, are

$$\frac{1}{P(h)} \simeq 1 + \frac{1}{3} h^2\, R_g^2 \qquad \text{(Zimm plot)} \quad (42)$$

and

$$\ln P(h) \simeq -\frac{1}{3} h^2\, R_g^2 \qquad \text{(Guinier plot)} \quad (43)$$

In the spirit of combining two or more solution properties into a shape-dependent quantity that does not depend on the particle size (Harding 1995), we propose here (we have not seen it in the literature) a combination of the two scattering-related properties, R_g and L, in the form of the ratio

$$H = \frac{L}{R_g} = \frac{L}{\sqrt{R_g^2}} \quad (44)$$

Two important typical values are $H = \sqrt{20/3} = 2.58$ for a solid sphere, and $H = \sqrt{12} = 3.46$ for a long rod (it should be noted that these values may not be the lowest and the highest bounds of H; for instance, $H = 2$ for a spherical shell and for a ring). The dispersion of these typical values suggests that H can be sensitive enough to macromolecular shape to be used for structural determination.

Covolume

Concentration dependence

At moderately low concentrations, the solution properties of macromolecules vary linearly with concentration, depending on the thermodynamic or hydrodynamic nonideality of the system (or both). In the case of the interpretation of thermodynamic equilibrium data (such as from sedimentation equilibrium distributions in the analytical ultracentrifuge, the angular intensity distribution of scattered light in classical or static light scattering measurements, or the osmotic pressure of a macromolecular solution), the concentration dependence coefficient is the second thermodynamic virial coefficient, B (or A_2) (ml mol/g^{-2}) given, for example, in terms of the apparent molecular weight at a finite concentration c (g/ml) by

$$\frac{1}{M_{\text{app}}} = \frac{1}{M} + \xi\, B\, c + \ldots \text{higher order terms in } c \ldots \tag{45}$$

where the concentrations are sufficiently low that the higher-order terms are ~0. For osmotic pressure, which depends directly on the number concentration of the macromolecular solute, $\xi = 1$; for Rayleigh or UV absorbance optical records of sedimentation equilibrium solute distributions, which depend directly on the weight concentration of the macromolecular solute, $\xi = 2$; for the angular intensity distribution of scattered light in classical or static light scattering, which also depends directly on the weight concentration of macromolecular solute, ξ also = 2. For Schlieren optical records of sedimentation equilibrium solute distributions, which depend directly on the weight concentration gradient, $\xi = 4$. [For a heterogeneous solute, M in Eq. (45) will be M_n for osmotic pressure, M_w for static light scattering and Rayleigh/UV absorbance sedimentation equilibrium, and M_z for Schlieren sedimentation equilibrium.] In the case of hydrodynamic transport properties such as the sedimentation coefficient and translational diffusion coefficient, the coefficient in concentration is not the thermodynamic second virial coefficient. In the case of the sedimentation coefficient it is the parameter k_s (ml/g) in

$$\frac{1}{s_{\text{app}}} \simeq \frac{1}{s}(1 + k_s\, c) \tag{46}$$

or

$$s_{\text{app}} \simeq s\,(1 - k_s\, c) \tag{47}$$

(Schachman 1959) and in the case of the translational diffusion coefficient it is the parameter k_d (ml/g) in

$$D_{\text{app}} \simeq D\,(1 + k_d\, c) \tag{48}$$

where

$$k_d = 2BM - \upsilon - k_s \tag{49}$$

(see Harding and Johnson 1985a). Thus B can also be experimentally obtained from measurement of k_d and k_s, and a good example of agreement between B measured from Eq. (49) and B from sedimentation equilibrium in the ultracentrifuge [Eq. (45) with $\xi = 2$] has been given for turnip yellow mosaic virus (Harding and Johnson 1985b).

Molecular covolume

The thermodynamic second virial coefficient B for a homogeneous, monodisperse solution of macromolecules depends on the size, shape, and polyelectrolyte properties of the macromolecular solute. It is usual (Tanford 1961; Ogston and Winzor 1975; Jeffrey et al. 1977; Nichol and Winzor 1985) to separate the combined contribution of size and shape (i.e. due to "excluded volume"), B_{ex}, from that of molecular charge:

$$B = B_{\text{ex}} + B_z \tag{50}$$

The most general expression for B_z for a macromolecular solute of charge (valency) z is:

$$B_z = [1000\, z^2/(4M^2 I)]\,[(1+2\,\kappa a_s)/(1+\kappa a_s)^2 + \ldots] \tag{51}$$

where I is the ionic strength (in mol/l), a_s is the equivalent Stokes radius of the (solvated) particle. κ (cm^{-1}) is the inverse Debye-Huckel screening length (Debye and Huckel 1923) and its magnitude may be evaluated from the expression $\kappa = 3.27\times10^7\sqrt{I}$ (I in mol/l) at 20 °C. At the isoelectric pH of a protein, z, and hence also, $B_z = 0$. At sufficiently high ionic strength, $(z, B_z) \to 0$.

The excluded volume contribution to the second virial coefficient, B_{ex}, is related to the excluded volume of a macromolecule or "molecular covolume" u (ml) by

$$B_{\text{ex}} = u\, N_A/(2M^2) \tag{52}$$

$$= U/(2M^2) \tag{53}$$

the product $u\,N_A$ is known as the "molar covolume" U (ml/mol). The molecular covolume, u, for impenetrable spherical particles has a simple interpretation: it is the volume of solution from which the centers of two molecules are mutually excluded. At non-zero but low concentrations the molecular covolume u is determined by pairwise, two-particle interactions.

In the most general case, the molecular covolume can be expressed in terms of an integral, given by

$$u = -K \int \left\{\exp\left[-\zeta(\boldsymbol{r}, \boldsymbol{\Omega})/kT\right] - 1\right\} \mathrm{d}^3\boldsymbol{r}\, \mathrm{d}^3\boldsymbol{\Omega} \tag{54}$$

$\zeta(\boldsymbol{r}, \boldsymbol{\Omega})$ is the interaction potential between two particles that depends on their relative positions, given by $\boldsymbol{r}$, and their relative orientations, given by $\boldsymbol{\Omega}$. We may fix one of the particles so that a specific center of it, C (for instance the center of mass), is at the origin of a lab-fixed system or coordinates, and with some specific system of axes (for instance, the main axes of inertia) aligned with the lab-fixed axes. The position of the second particle with respect to the first one is specified by the position vector of the point C of particle 2 with respect to point C of particle 1.

K in Eq. (54) is a normalization constant such that $K\int \mathrm{d}^3\boldsymbol{\Omega} = 1$. The orientation of particle 2 with respect to particle 1 (axes x_2, y_2, z_2 with respect to axes x_1, y_1, z_1) can be characterized, in the most general case, in terms of three Euler angles, $\boldsymbol{\Omega} = (\theta, \phi, \psi)$. Thus, the integral in Eq. (54) is sextuple, involving the three coordinates of $\boldsymbol{r}$ and the three Euler angles. For instance:

- $\boldsymbol{r}$ in Cartesian coordinates (x, y, z); $\boldsymbol{\Omega}$ in Euler angles:

$$K\int\ldots \mathrm{d}^3\boldsymbol{r}\ \mathrm{d}^3\boldsymbol{\Omega} = \frac{1}{8\pi^2}\int\ldots \mathrm{d}x\ \mathrm{d}y\ \mathrm{d}z \sin\theta\ \mathrm{d}\theta\ \mathrm{d}\phi\ \mathrm{d}\psi \qquad (55)$$

- $\boldsymbol{r}$ in spherical coordinates (r, θ, ϕ); $\boldsymbol{\Omega}$ in Euler angles:

$$K\int\ldots \mathrm{d}^3\boldsymbol{r}\ \mathrm{d}^3\boldsymbol{\Omega} = \frac{1}{8\pi^2}\int\ldots r^2 \sin\theta'\ \mathrm{d}r\ \mathrm{d}\theta'\ \mathrm{d}\phi' \sin\theta\ \mathrm{d}\theta\ \mathrm{d}\phi\ \mathrm{d}\psi \qquad (56)$$

The above expressions are normalized to the set of Euler angles setting $K = 1/(8\pi^2)$:

$$\frac{1}{8\pi^2}\int_{\theta=0}^{\pi}\int_{\phi=0}^{2\pi}\int_{\psi=0}^{2\pi} \sin\theta\ \mathrm{d}\theta\ \mathrm{d}\phi\ \mathrm{d}\psi = 1 \qquad (57)$$

In the case of asymmetric particles, it would be possible to express $\boldsymbol{\Omega}$ in terms of only the two polar angles $\theta \in (0, \pi)$ and $\phi \in (0, 2\pi)$, with a normalization constant $K = 1/(4\pi)$.

Now, regarding the interaction potential, it is assumed to have a simple form for particles whose only interaction consists of just forbidding overlapping, i.e., $\zeta(\boldsymbol{r}, \boldsymbol{\Omega}) = \infty$ if the particles overlap and $\zeta(\boldsymbol{r}, \boldsymbol{\Omega}) = 0$ if they do not.

Then, the molecular covolume is

$$u = -K\int f_{12}(\boldsymbol{r}, \boldsymbol{\Omega})\, \mathrm{d}^3\boldsymbol{r}\ \mathrm{d}^3\boldsymbol{\Omega} \qquad (58)$$

where $f_{12}(\boldsymbol{r}, \boldsymbol{\Omega}) = -1$ or 0 depending on whether particles 1 and 2 overlap or not. The simplest example is that of spherical particles of radius a. The problem is orientation-independent, and the triple integration over Euler angles reduces trivially to the normalization condition [Eq. (57)]. Furthermore, the remaining integration over $\boldsymbol{r}$ reduces to the region where $f_{12} = 1$, which is a sphere of radius $2a$. The integration is carried out in spherical coordinates [Eq. (56)], and we finally obtain the covolume of spherical

$$u = -\int_{\phi'=0}^{2\pi}\int_{\theta'=0}^{\pi}\int_{r=0}^{2a} (-1)\cdot r^2 \sin\theta'\ \mathrm{d}r\ \mathrm{d}\theta'\ \mathrm{d}\phi' = \frac{4}{3}\pi(2a)^3 = 8V \qquad (59)$$

where V is the volume of the (solvated) particle. The most general rigid particle shape for which u has been worked out is that for (pairwise interactions) involving general triaxial ellipsoids at dominant Brownian motion where all orientations are equally probable. This was studied by Rallison and Harding (1985), who followed a scheme outlined for general particles earlier by Isihara (see Isihara 1950; Hirschfelder et al. 1954; Yamakawa 1971). The general expression is

$$u = 2V + 2RS \qquad (60)$$

where R and S are both double integrals. Although it is possible to evaluate one of the integrals in each double integral analytically, the results are so complicated as to be opaque, so it is as easy to evaluate the whole double integral in both R and S numerically, and this can be done using standard packages of Harding et al. (1997) and Harding (1998).

Estimation of u for arbitrary particles using a Monte Carlo procedure

For the evaluation of the sextuple integral involved in the calculation of u [Eq. (54) or (58)] we propose a simple Monte Carlo recipe, which is inspired in the fact that the integrand f_{12} can only take one of two values, 0 or 1.

We first set particle 1 in a convenient position and orientation. The particle is rotated in such a way that the longest distance vector within the particle, $\boldsymbol{L}$ (whose modulus L_z is the longest chord), is parallel to axis z. A standard transformation based on Euler angles is employed for obtaining the bead coordinates after this step. Next, the longest dimensions in the x and y directions, L_x and L_y, are obtained. Thus, the particle is enclosed in a parallelepipedic cage with sides L_x, L_y, and L_z. Then, the center, P, of the cage is determined and the coordinates are translated to a system of axes with the origin at P. The half-dimensions of the cage centered at P are $L_x/2$, $L_y/2$, and $L_z/2$; the longest dimension of the cage is the diagonal, $D = (L_x^2 + L_y^2 + L_z^2)^{1/2}$.

The positions and random orientations of particle 2 can be obtained by translating particle 1 from P to Q [thus $\boldsymbol{r}$ in Eqs. (54)–(58) would be the $\boldsymbol{PQ}$ vector] and rotating the coordinates with a uniformly random set of Euler angles, Ω in Eqs. (54)–(58); $\cos\theta$ is uniformly random in $(-1, 1)$ and ϕ and ψ are uniformly random in $(0, 2\pi)$. It is clear that the two particles cannot overlap if their respective cages do not overlap either. Overlap is not possible if center Q of particle 2 is outside a parallelepiped centered at P with sides $2X = L_x + D$, $2Y = L_y + D$, $2Z = L_z + D$. Therefore, we restrict the Monte Carlo sampling to position Q with coordinates (x_Q, y_Q, z_Q) that are uniformly distributed random numbers in the intervals $(-X, +X)$, $(-Y, +Y)$, $(-Z, +Z)$, respectively. The volume of such region is $V_{\mathrm{region}} = 8XYZ$.

For the generated $\boldsymbol{r}$ and $\boldsymbol{\Omega}$, it is checked whether or not the particles overlap. This condition can be easily programmed since our particles are bead models: particles overlap if any two beads overlap. A very large number of such trials, N_{trials}, are made, of which N_{overlap} result in overlapping. Then, the molecular covolume is given by

$$u = \frac{N_{\mathrm{overlap}}}{N_{\mathrm{trials}}} V_{\mathrm{region}} \qquad (61)$$

and the reduced covolume u_{red} is therefore

$$u_{red} = [N_{overlap}/N_{trials}] \cdot [V_{region}/V] \quad (62)$$

Tests of the procedure

We have checked the performance of our Monte Carlo procedure in SOLPRO for covolume, applying it to some simple cases where the result is known: ellipsoids (including the sphere) and cylindrical rods.

For a single sphere, the exact result is $u = 8V$, where V is the volume of the sphere. With only 60 000 Monte Carlo trials, we obtain $u/V = 8.0 \pm 0.3$. If the number of trials is 10^7, we obtain $u/V = 7.998$. The excellent accuracy and efficiency of our procedure is due to the compactness of the sphere, but not to its spherical symmetry. Indeed, a similar performance can be expected for nearly isometrical, globular particles.

A more difficult situation for our procedure occurs with elongated particles. It is clear that, for slender bodies, V_{region} is much larger than the particle's volume. As a consequence, the "hit ratio" in the Monte Carlo procedure ($N_{overlap}/N_{trials}$) is quite small, and therefore the statistical (relative) error in its determination is large. The statistical error can be reduced by increasing N_{trials}, but this has the obvious cost of increasing the CPU time. Furthermore, bead models of elongated particles usually have a large number of beads, N, and the CPU time required for checking overlap in each trial increases with N^2.

The second virial coefficient and covolume of cylindrical rods can be calculated from simple expressions. For very long rods, when the length L is much larger than the diameter, d, the limiting result was given by Zimm (see Yamakawa 1971): $u = \pi L^2 d/2$. For not too long rods, the following result is available (Isihara 1950; Hirschfelder et al. 1954; Yamakawa 1971)

$$u = \frac{\pi L^2 d}{2}\left[1 + \frac{(3+\pi)}{2}\left(\frac{d}{L}\right) + \frac{\pi}{4}\left(\frac{d}{L}\right)^2\right] \quad (63)$$

which tends to the Zimm result in the $L/d \to \infty$ limit. We model rods as straight strings of N touching (i.e., tangent, non-overlapping) beads of identical size, with radius σ, so that $L = 2\sigma N$. There is some ambiguity in the correspondence between the cylinder diameter d and the diameter of the beads, 2σ. A first possibility, method A, is making $d = 2\sigma$, $\sigma = 0.5\,d$, so that the bead model is inscribed within the cylinder. This model underestimates the volume of the particle, and one may think that it would therefore underestimate its covolume. Second, in method B the volume of the bead model is equalized to that of the particle, making $\sigma = 0.613\,d$. Covolume is not strictly related to the particle's volume, but rather to the volume that it excludes, and thus the thickness of the bead model can be regarded in terms of the minimum distance of separation between the axes to two side-by-side touching rods. As one rod of beads slides along the other, this distance varies from 2σ to 1.732σ, and the proper (geometric) average, 1.92σ, is taken as the equivalent cylinder diameter, so that $\sigma = 0.521\,d$.

Table 1 Covolume of cylindrical rods: Monte Carlo results from SOLPRO and comparison with theoretical results

$p = L/d$	$N_{trials} = 10^7$ u_{MC}	N_{trials} variable		u_{MC}/u_{theor} methods		
		N_{trials}	u'_{MC}	A	B	C
5	50.5	5×10^4	50.7±0.3	0.781	0.827	1.028
10	173.6	2×10^5	174.6±1.1	0.841	0.884	1.072
20	637.6	3×10^5	639±7	0.878	0.920	1.098
30	1 397.6	5×10^5	1 390±10	0.896	0.937	1.112
50	3 777.7	8×10^5	3 770±40	0.906	0.946	1.117
100	14 897.4	1×10^6	14 800±100	0.920	0.960	1.128

In Table 1 we list simulated and theoretical values of covolume. We present results obtained from SOLPRO with a very large N_{trials} (affected by a negligible error), that are employed for the comparison with theory, and results with a moderate N_{trials}, showing their statistical error. The latter required a quite reasonable CPU time; the worst case, $L/d = 100$ took 50 min of CPU time on a Pentium 200 personal computer. The N_{trials} values were such that the resulting statistical errors are about 1%. The ratios of simulated-to-theoretical values, given in Table 1 for the three models, approach unity in all cases. For short rods, method C is better, while for longer rods the best result is found for method B. Anyhow, the ratios are in most cases between 0.9 and 1.1; in other words, the deviation of the SOLPRO results from the exact ones is typically under 10%.

We have made a similar study for prolate ellipsoids; covolume is given by an exact expression (Isihara 1950; Yamakawa 1971) and can be readily evaluated using the ELLIPS2 program (Harding et al. 1997). As for the previous problem, there is some ambiguity in defining the bead model. Method A is as proposed by Bloomfield et al. (1967): the model is a string of colinear beads with different radii, decreasing from the center toward the ends, and has the same length, $2a$, as the true ellipsoid, in which the bead model is inscribed. Method B is a volume-equalized modification of the former (García de la Torre and Bloomfield 1977): the bead model is constructed with an ellipsoidal envelope with semiaxes (a, b', b'), with b' such that the volume of the model is the same as the (a, b, b) ellipsoid. The results are given in Table 2, with a presentation similar to that in Table 1 for rods. The results calculated with a moderate N_{trials} follow a trend similar to that for rods (actually, we report this for one of the methods). Also, the simulation-to-theoretical ratios behave like those for rods: while the inscribed model underestimates the covolume (–9%), the volume-equalized model overestimates it (+13%), with deviations of roughly 10%, as for rods. From the empirical findings with models A and B, we note that if one would take the simple mean of the results with and without volume equalization, the final result would be very close to the theoretical one.

Table 2 Covolume of ellipsoids: Monte Carlo results from SOLPRO and comparison with theoretical results

$p = a/b$	Model not equalized				Model equalized			
	$N_{trials} = 10^7$ u_{MC}	N_{trials} variable			$N_{trials} = 10^7$ u_{MC}	N_{trials} variable		
		N_{trials}	u'_{MC}	Ratio		N_{trials}	u'_{MC}	Ratio
1	33.5	6×10^4	33.8±0.4	0.999	33.5	6×10^4	33.8±0.4	0.999
2	59.6	4×10^4	59.1±0.5	0.784	77.3	4×10^4	76.4±0.7	1.017
3	114.9	4×10^4	114.3±0.7	0.838	158.7	4×10^4	157.7±1.5	1.158
5	280.5	5×10^4	280±3	0.887	361.1	5×10^4	360±2	1.141
10	999.9	1.2×10^5	1 007±9	0.905	1 258.1	1.2×10^5	1 266±11	1.138
20	3 796.3	3.7×10^5	3 810±30	0.913	4 707.7	3.5×10^5	4 720±40	1.133
30	8 442.3	3.5×10^5	8 450±60	0.920	10 409.6	3×10^5	10 490±90	1.134
50	23 233.8	8×10^5	23 300±200	0.924	28 444.4	4×10^5	28 600±200	1.132
100	92 149.1	1×10^6	92 100±900	0.925	112 479.5	2×10^6	111 700±500	1.139

Covolume-based shape-dependent quantities

Dimensionless quantities that combine covolume and other solution properties can be formulated in such a way that they behave as shape-functions, depending on the shape of the particle but not on its actual size. A very simple combination is the ratio of covolume, u, to the volume, V of the particle; it is the so-called reduced molecular volume:

$$u_{red} = \frac{u}{V} \tag{64}$$

For the sphere, $u_{red} = 8$, while for a very long rod, $u_{red} = 2L/d$.

The determination of the effective volume for a particle in solution is not a trivial problem, owing to hydrodynamic effects (as seen above for bead models of ellipsoids and rods) or hydration (vide infra). Therefore, it is safer to combine covolume with hydrodynamic properties, and two compound quantities have been formulated: the ψ function of Jeffrey et al. (1977), combining u_{red} with a translational property, and the Harding's Π function (Harding 1981) that combines u_{red} with the intrinsic viscosity. These functions are formulated as:

$$\psi = \frac{u_{red}}{162\,\pi^2}\,P^{-3} \tag{65}$$

$$\Pi = \frac{u_{red}}{\nu} \tag{66}$$

In Eq. (65), $P = f/f_0$ is the Perrin function, where f is the translational friction coefficient of the particle and f_0 is that of a sphere of the same volume. In Eq. (66), ν is the so-called viscosity increment (Einstein function), such that the intrinsic viscosity $[\eta] = \nu\,\bar{v}$, where $\bar{v}$ is the particle's partial specific volume.

The present version of SOLPRO combines the value of the covolume of the bead model with the volume calculated for it, $V = (4/3)\,\pi \sum \sigma_i^3$, to obtain u_{red}. The covolume is also combined with the hydrodynamic properties, obtained in HYDRO or elsewhere and passed to SOLPRO, to evaluate the ψ and Π functions.

Example of HYDRO/SOLPRO calculation

As an example of the use of SOLPRO, we present the results of a calculation on a typical bead model, corresponding to the human immunoglobulin antibody molecule IgG3, proposed by Gregory et al. (1987), which was already employed as an example in previous descriptions of HYDRO (García de la Torre et al. 1994) and SOLPRO (García de la Torre et al. 1997). This model is depicted in Fig. 1. In Fig. 2 we reproduce some parts of the output produced from SOLPRO when the printing option is activated (IPRIN=1). We only reproduce those parts related to the new features of SOLPRO.

We first notice that SOLPRO calculates the radius of gyration and volume of the model in the same way as HYDRO. The reasons for repeating here the calculations are that SOLPRO may be used without a previous call to HYDRO (for instance, if one wishes to obtain only scattering quantities), or because the model submitted to SOLPRO may be different from that used in HYDRO if one is considering particular effects such as hydration (see below).

For the calculation of properties related to NMR relaxation, the dipole was arbitrarily taken along the axis of the Fab subunits. The ranges of time and frequency, for $P_2(t)$ and $J(\omega)$, respectively, are taken as 4 τ_1 and 4 τ_1^{-1}, using an "automatic" setting of the program, where τ_1 is the longest of the five relaxation times. These two functions are plotted in Fig. 3.

The distribution of distances, $p(r)$, calculated from SOLPRO is plotted in Fig. 4. For the sake comparison, we have included also in Fig. 4 the distribution of distances for a spherical particle having the same radius of gyration as IgG3. Thus the effect of elongated shape on $p(r)$ can be appreciated. This effect is noticed in the value of the compound activity, $H = 2.887$, which deviates from the value for a sphere, $H = 2.582$.

In Fig. 5 we present graphs of the scattering form factor, $P(h)$. We have repeated that calculation as in our previous paper just to correct an error arising from a bug detected in that part of the computer code.

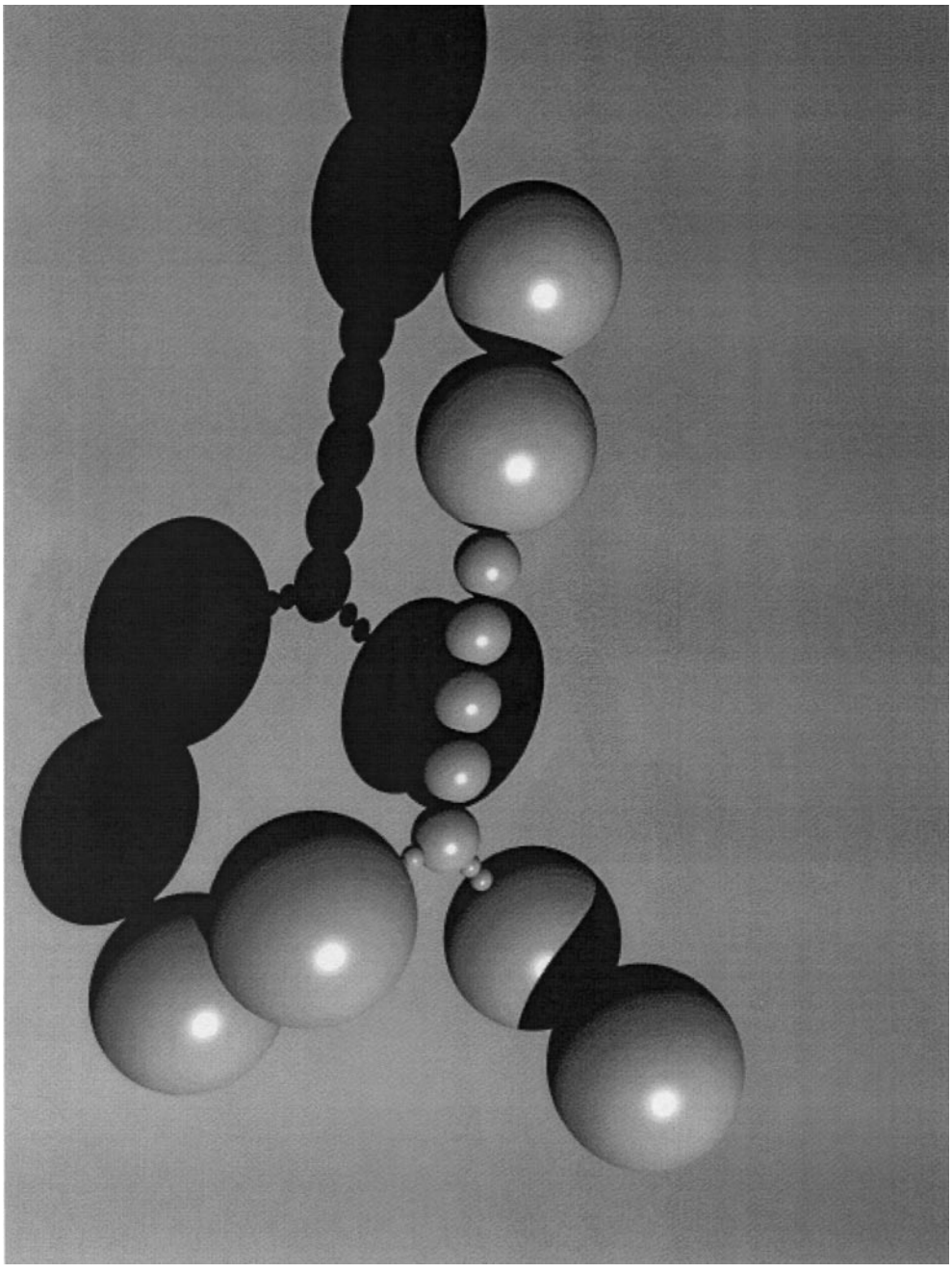

Fig. 1 Model for the human immunoglobulin IgG3, according to Gregory et al. (1987)

Regarding the results for covolume, one should keep in mind that the open (non-compact) and elongated shape of IgG3 requires a large number of N_{trials} to reach a reasonably low statistical error. With $N_{\text{trials}} = 600\,000$ (which only took about 1 min on a Pentium 200 PC), we obtained $u = 6690 \pm 30$ Å^3, with an error of about 0.5%.

Other aspects

There are some aspects of the calculation of primitive or compound solution properties that are implicit in hydrodynamic theory and in bead modeling strategies. We mention here two of such aspects, giving some guidelines or warnings to the SOLPRO user.

Bead overlapping

Hydrodynamic theory and computer algorithms for bead modeling (HYDRO) have been devised for assemblies of *non-overlapping* spheres. Such must be the case for quantities such as the bead friction coefficient and the modified hydrodynamic interaction tensor to by physically correct. HYDRO contained a patch to avoid a program

```
                  IMMUNOGLOBULIN IGG3
                     Number of beads  15
  Translational diffusion coefficient  3.821E-07 cm2/s
       Radius of gyration(from HYDRO)  7.492E-07 cm
                  Volume(from HYDRO)  2.256E-19 cm3
                Relaxation time (1)  4.321E-07 s
                Relaxation time (2)  3.445E-07 s
                Relaxation time (3)  3.287E-07 s
                Relaxation time (4)  2.024E-07 s
                Relaxation time (5)  2.023E-07 s
           Harmonic relaxation time  2.756E-07 s
                Intrinsic viscosity  9.823E+00 cm3/g
          Sedimentation coefficient  5.826E+00 svedberg

              Volume(from SOLPRO)=  2.256E-19 cm3
     Radius of gyration(uncorrected,
                    from SOLPRO)=   7.328E-07 cm
       Radius of gyration(corrected,
                    from SOLPRO)=   7.492E-07 cm
(The corrected Rg includes the correction from bead size)
                  Longest chord =  2.163E-06 cm
                          ***************
  Initial relaxation time ratio (nmr)  7.616E+00
     Mean relaxation time ratio (nmr)  7.674E+00
                          ***************
        Ktaur initial function (nmr)  2.461E+24
           Ktaur mean function (nmr)  2.480E+24
                          ***************
          Psi initial function (nmr)  7.684E-01
             Psi mean function (nmr)  7.665E-01
                          ***************
       Lambda initial function (nmr)  1.500E+00
          Lambda mean function (nmr)  1.488E+00
                          ***************

EIGEN-ANALYSIS OF ROTATIONAL DIFFUSION
 EIGENVALUE   EIGENVECTOR
 1.663E-03     6.093E-08  7.480E-01 -6.637E-01
 1.876E-03     1.848E-08  6.637E-01  7.480E-01
 4.777E-03     1.000E+00 -5.784E-08  2.662E-08


CALCULATION OF P2 CORRELATION FOR DIPOLAR NMR

COUPLING DIPOLE VECTOR (unitary)
 In user´s axes
 5.000E-01 -8.660E-01  0.000E+00
 In rotational diffusion axes
 1.447E-08 -2.008E-01 -9.796E-01


                 RELAXATION
K    AMPLITUDE      TIME
1    8.799E-01    4.321E-07
2    1.161E-01    3.445E-07
3    6.026E-16    3.287E-07
4    2.531E-17    2.024E-07
5    4.093E-03    2.023E-07
```

```
INITIAL RELAXATION TIME FOR P2 - NMR:  4.178E-07
   MEAN RELAXATION TIME FOR P2 - NMR:  4.210E-07

   TIME     VALUE OF P2
 0.000E+00    1.000E+00
 1.728E-08    9.595E-01
 3.457E-08    9.206E-01
       ...........
       ...........
       ...........
 1.694E-06    1.831E-02
 1.711E-06    1.758E-02
 1.728E-06    1.688E-02

CALCULATION OF VALUES OF SPECTRAL DENSITY FUNCTION
FRECUENCY    SPEC.DENS.
 0.000E+00    4.210E-07
 9.257E+04    4.203E-07
 1.851E+05    4.184E-07
       ...........
       ...........
       ...........
 9.072E+06    2.713E-08
 9.164E+06    2.662E-08
 9.257E+06    2.613E-08

DISTRIBUTION OF DISTANCES

INTERVALS BETWEEN RMIN AND RMAX, CENTERED AT R;
VALUES OF p(R)


  RMIN(cm)     RMAX(cm)      R(cm)     p(R)(cm^(-1))
  0.000E+00   7.211E-08   3.605E-08   6.240E+04
  7.211E-08   1.442E-07   1.082E-07   3.980E+05
  1.442E-07   2.163E-07   1.803E-07   7.262E+05
        ..............................
        ..............................
  1.947E-06   2.019E-06   1.983E-06   8.623E+04
  2.019E-06   2.091E-06   2.055E-06   2.417E+04
  2.091E-06   2.163E-06   2.127E-06   1.129E+03

Check for normalization:
(RMAX-RMIN)*SUM(p(R))=  9.996E-01  SHOULD BE= 1


MONTE CARLO SIMULATION OF COVOLUME OF BEAD MODELS
NUMBER OF TRIALS=     10000 DIVIDED INTO 10 SUBSETS


FINAL RESULT: COVOLUME=  6.737E-18 +-  1.982E-19 cm3
```

Fig. 2 Parts of the output from SOLPRO, from the new calculations in the latest version. Parts from the calculations in the previous version (*marked with asterisks*) have been removed

abortion or severe numerical errors that may occur if two beads would occasionally overlap due to minor modeling errors or physical assumptions (as in the simulation of random-flight flexible chains). However, some authors have employed bead models with systematic (sometimes intensive) overlap. It would be convenient to have hydrodynamically adequate ways to cope with bead overlapping but the problem is still under consideration (Carrasco 1998).

The calculation in SOLPRO of other, non-hydrodynamic solution properties is based, again, on the assumption of non-overlapping beads. Thus, our theoretical development of distance distribution is only valid in such a case. The radius of gyration and, mostly, the particle (model) volume itself are also calculated in such an assumption. Therefore, it is recommended that HYDRO and SOLPRO will be used for bead models without overlapping. We recall that in a pair of touching but non-overlapping spheres, the fluid between them, around the point of tangency, is hydrodynamically trapped, so that the tangent pair has indeed a region of hydrodynamic overlap.

Hydration

Macromolecular hydration has not been explicitely considered either in HYDRO or in SOLPRO. Of course, the bead model employed for calculation of hydrodynamic properties in HYDRO should include the user's view of hydration. However, some of the properties calculated in SOLPRO may not be affected by hydration. Such is the case of the scattering-dependent properties, if one assumes that scattering does not distinguish hydration water from bulk water.

The difficulty regarding hydration is that its influence on the particle shape depends on the shape itself. Basically, we differentiate two schemes to treat hydration, as described below.

The uniform expansion

In the uniform expansion scheme, we assume that the shape of the hydrated particle is the same as that of the dry parti-

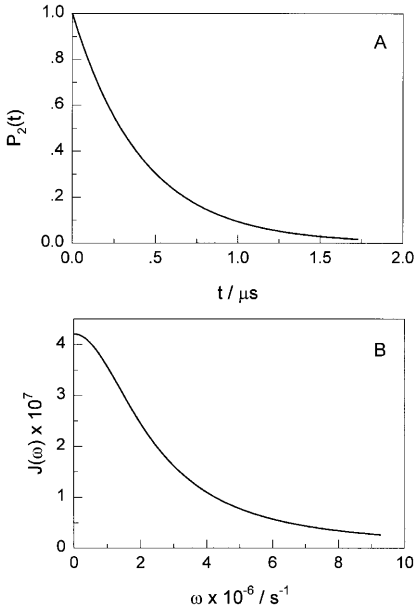

Fig. 3A, B NMR relaxations functions calculated for IgG3 with a dipole along the Fab subunit: **A** $P_2(t)$; **B** $J(\omega)$

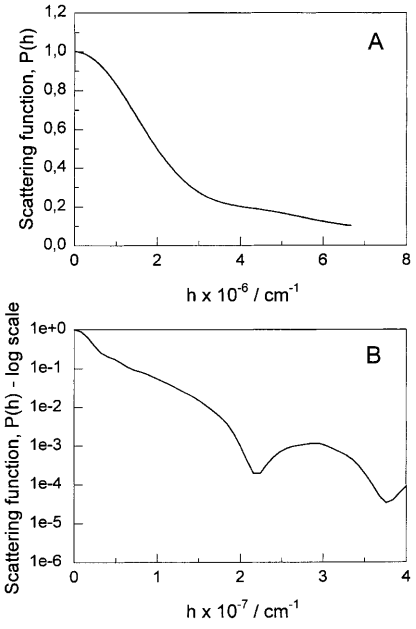

Fig. 5A, B Scattering function calculated for the bead model of IgG3: **A** Low-angle scattering; **B** wide angle-scattering

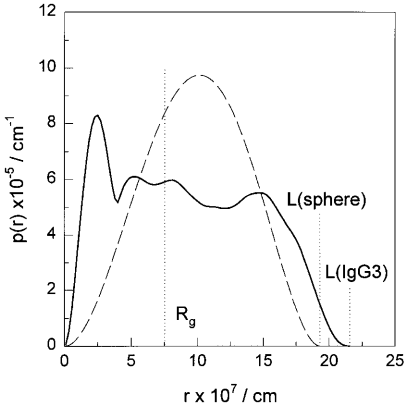

Fig. 4 Distribution of distances, $p(r)$, for the IgG3 model. The $p(r)$ function for a sphere (*dashed line*) having the same R_g=74.92 Å as IgG3 (*continuous line*) is represented. R_g and L for IgG3 and the sphere are marked

cle, with the only difference of a uniform change in size. This assumption is acceptable when the particle is compact (without large cavities that would act as "water pockets"), and not too anisometric, so that the relative size increases of any linear dimension due to the hydration layer is roughly the same in any direction, and can be expressed as

$$h = \left(1 + \frac{\delta}{\bar{v}\,\rho}\right)^{1/3} \tag{67}$$

where δ is the hydration degree. This scheme is the same as the classical procedure for describing macromolecular properties in terms of hydrated ellipsoids (Tanford 1961) and it is has been devised with globular proteins in mind. In the case of ellipsoids, it is assumed that the anhydrous and the hydrated particle have the same axial ratio.

In a general case, if p_{hyd} and p_{anh} are the values of any solution property, corresponding respectively to the hydrated and anhydrous particle, in the present hypothesis of uniform expansion they are related by:

$$p_{hyd} = h^n\, p_{anh} \tag{68}$$

where the exponent n reflects the dependence of the property on linear size. For the compound quantities (shape function), n will be a combination of those for the involved properties. When those properties are all hydrodynamic (including covolume), the shape functions are defined, from the early studies of ellipsoids, in such a way that they are independent of the degree of hydration. Otherwise, a correction for hydration must be applied.

On the assumption that the scattering-related properties, R_g and L, and the volume entering in some compound properties correspond to the dry particle, then the practical procedure that we propose for the uniform expansion case is as follows:

1. Devise a hydrodynamic model whose size and shape already *includes hydration* and call HYDRO to obtain the hydrodynamic quantities.

2. Call SOLPRO, passing to it the *same "hydrated" model* along with the HYDRO result.

3. Correct (by hand after the computer calculation, or making a change in the computer program) some of the SOLPRO results, multiplying by the following factors, R_g, h^{-1}; L, h^{-1}; V, h^{-3}. On the other hand, D_t, f, τ', and $[\eta]$ remain unchanged.

According to some authors (Kumosinski and Pessen 1985), certain types of scattering techniques "see" somehow the particle's hydration, distinguishing between bound water and water in the bulk. In the present, uniform expansion assumption, an adequate way to treat such a sit-

uation consists of applying a different expansion factor, t, to the scattering related properties. Typically, $1 \leq t \leq h$, with $t = 0$ if scattering were insensitive to hydration. In the above-mentioned scheme for calculations, some corrections would be different, particularly: R_g, t/h; L, t/h.

When hydration is present, the handling of the shape-dependent functions P, ν, β, G, etc. should be made with care, accounting for the hydration effect in the obtention of the experimental values of these functions; for details, see Carrasco et al. (1998).

The non-uniform expansion

The uniform expansion hypothesis is extremely inadequate in certain circumstances, particularly for elongated structures such as DNA pieces, fibrous proteins, etc. Let us consider the example of a rod-like fibrous protein with L = 1400 Å and d = 20 Å (anhydrous), with $\bar{v} = 0.7$ cm^3/g and a hydration degree $\delta = 0.3$ g/g, so that the expansion factor would be $h^3 = 1.43$, $h = 1.13$. If expansion were uniform, the hydrated length of the protein would be 1630 Å, with an increase in length of over 200 Å, which is absolutely unreasonable. The proper approach in this example is to assume a layer of water of a few Å around the protein. The relative increase in length is negligible, but the relative increase in diameter is appreciable. If the expansion is attributed to the radial directions only, then the hydrated diameter would be $20\sqrt{1.43} = 24$ Å, which seems quite reasonable.

It is therefore clear that, when expansion due to hydration is not uniform, the dry and the hydrated shapes are not the same, and therefore slightly different bead models must be used. In the above example, the dry protein would be a string of 70 beads of diameter 20 Å (inscribed model; see section on Tests of the procedure, above), while the hydrated protein would be modeled with about 59 beads of about 24 Å. In the general case, the hydrated model would be used for the HYDRO calculation. The results would passed in the subsequent call SOLPRO, but with the coordinates of the anhydrous model.

It should be pointed out that both of the above procedures to account for hydration are approximate and not strictly correct, particularly when applied to scattering calculations. Both the uniform and the non-uniform procedures do not account for the different and fluctuating scattering density of water in the hydration layer [for a recent study of hydration effects in scattering, see Svergun et al. (1998)]. Thus the procedures should be applied with caution to model scattering-related properties when hydration is important in relative terms; this may be the case for some globular proteins. In other instances, including large proteins and macromolecular complexes, hydration may be relatively less important, with the scattering being mainly determined by the size and shape of the macromolecular material. In regard to hydrodynamic properties, the possibilities of choosing one or the other procedure, along with the choice of the h and t factors in the uniform expansion method, seemingly cover well all the application. At any rate, these procedures are the only feasible ways to include hydration in both hydrodynamics and scattering in the common methodological framework of bead modeling.

Computer programs

Both HYDRO and SOLPRO are public domain programs, with the form of FORTRAN subroutines which will be linked to the user's main program. The source code for both subroutines is freely available, so that calculations can be customized to deal with any specific effect (hydration, for instance) or modeling needs. For users who wish to avoid programming, or if a FORTRAN compiler is not available, we supply also executables for various computers. All the program files and further information can be found on the internet www page http://leonardo.fcu.um.es/macromol.

Acknowledgements This work has been supported by grant PB96-1106 from the Dirección General de Enseñanza Superior, M. E. C. (Spain). B. C. is the recipient of a predoctoral fellowship from the same source. Support from the B. B. S. R. C. (UK) is also acknowledged.

References

Abragam A (1961) The principles of nuclear magnetism. Clarendon Press, Oxford

Barbato G, Iruka M, Kay LE, Pastor RW, Bax A (1992) Backbone dynamics of calmodulin studied by ^{15}N relaxation using inverse detected two-dimensional NMR spectroscopy: the central helix is flexible. Biochemistry 16: 5269–5278

Birchall AJ, Lane AN (1990) Anisotropic rotation in nucleic acid fragments: significance for determination of structures from NMR data. Eur Biophys J 19: 73–78

Bloomfield VA, Dalton WO, Holde KE van (1967) Frictional coefficients of multisubunit structures. I. Theory. Biopolymers 5: 135–148

Carrasco B (1998) PhD thesis, Universidad de Murcia, Spain

Carrasco B, Harding SE, García de la Torre J (1998) Bead modeling using HYDRO and SOLPRO of the conformation of multisubunit proteins: sunflower and rape-seed 11S globulins. Biophys Chem (in press)

Clore GM, Driscoll PC, Wingfield PT, Gronenborn A (1990) Analysis of backbone dynamics of interleukin-1β using two-dimensional inverse detected heteronuclear ^{15}N-^{1}H NMR spectroscopy. Biochemistry 29: 7387–7401

Debye P, Huckel E (1923) The theory of electrolytes. 1. Lowering of freezing point and related phenomena. Phys Z 24: 185–206

Eimer WJ, Williamson J, Boxer S, Pecora R (1990) Characterization of the overall and internal dynamics of short oligonucleotides by depolarized light scattering and NMR relaxation measurements. Biochemistry 29: 799–811

Evans JS (1995) Biomolecular NMR spectroscopy. Oxford University Press, Oxford

Favro LD (1960) Theory of the rotational Brownian motion of a free rigid body. Phys Rev 119: 53–62

García de la Torre J (1989) Hydrodynamic properties of macromolecular assemblies. In: Harding SE, Rowe AJ (eds) Dynamic properties of macromolecular assemblies. Royal Society of Chemistry, Cambridge, pp 3–31

García de la Torre J, Bloomfield VA (1977) Hydrodynamic properties of macromolecular complexes. I. Translation. Biopolymers 16: 1747–1763

García de la Torre J, Bloomfield VA (1981) Hydrodynamic properties of complex, rigid, biological macromolecules. Theory and applications. Q Rev Biophys 14:81–139

García de la Torre J, Navarro S, López Martínez MC, Díaz FG, López Cascales JJ (1994) HYDRO: a computer software for the prediction of hydrodynamic properties of macromolecules. Biophys J 67:530–531

García de la Torre J, Carrasco B, Harding SE (1997) SOLPRO: theory and computer program for the prediction of SOLution PROperties of rigid macromolecules and bioparticles. Eur Biophys J 25:361–372

Glatter O, Kratky O (1982) Small angle X-ray scattering. Academic, New York

Gregory L, Davis KS, Sheth B, Boyd J, Jefferis R, Naves C, Burton D (1987) The solution conformation of the subclass of human IgG deduced from sedimentation and small-angle x-ray scattering. Mol Immunol 24:821–829

Harding SE (1981) A compound hydrodynamic shape function derived from viscosity and molecular covolume measurements. Int J Biol Macromol 3:340–342

Harding SE (1995) On the hydrodynamic analysis of macromolecular conformation. Biophys Chem 55:69–93

Harding SE (1998) The intrinsic viscosity of biological macromolecules. Progress in measurement, interpretation and application to structures in dilute solution. Prog Biophys Mol Biol (in press)

Harding SE, Johnson P (1985a) The concentration dependence of macromolecular parameters. Biochem J 231:543–547

Harding SE, Johnson P (1985b) Physicochemical studies on turnip yellow mosaic virus: homogenity, molecular weights, hydrodynamic radii and concentration dependence of parameters. Biochem J 231:549–555

Harding SE, Horton JC, Colfen H (1997) The ELLIPS suite of macromolecular conformation algorithms. Eur Biophys J 25:347–360

Hirschfelder JO, Curtis CF, Bird RB (1954) Molecular theory of gases and liquids. Wiley, New York

Huntress WT (1968) Effects of anisotropic molecular rotational diffusion on nuclear magnetic relaxation in liquids. J Chem Phys 48:3524–3533

Isihara A (1950) Determination of molecular shape by osmotic measurement. J Chem Phys 18:1446–1449

Jeffrey PD, Nichol LW, Turner DR, Winzor DJ (1977) The combination of molecular covolume and frictional coefficients to determine the shape and axial ratio of a rigid macromolecule: studies on ovalbumin. J Phys Chem 81:776–781

Kumosinski T, Pessen H (1985) Structural interpretation of hydrodynamic measurements of proteins in solution through correlations with x-ray data. Methods Enzymol 117:154–182

Nichol LW, Winzor DJ (1985) The use of covolume in the estimation of protein axial ratios. Methods Enzymol 117:183–199

Nuutero S, Fujimoto B Flynn P, Reid R, Ribeiro N, Schurr JM (1994) The amplitude of local angular motions of purines in DNA in solution. Biopolymers 34:463–480

Ogston AG, Winzor DJ (1975) Treatment of thermodynamic nonideality in equilibrium studies on associating solutes. J Phys Chem 79:2496–2500

Palmer AG, Williams J, McDermott A (1996) Nuclear magnetic resonance studies of biopolymer dynamics. J Phys Chem 100:13293–13310

Rallison JM, Harding SE (1985) Excluded volumes for pairs of triaxial ellipsoids at dominant Brownian motion. J Colloid Interface Sci 103:284–289

Schachman HK (1959) Ultracentrifugation in biochemistry. Academic Press, New York

Svergun DI, Richard S, Koch MHJ, Sayers Z, Kuprin S, Zaccai G (1998) Protein hydration in solution: experimental observation by x-ray and neutron scattering. Proc Natl Acad Sci USA 95:2267–2272

Tanford C (1961) Physical chemistry of macromolecules. Wiley, New York

Tjandra N, Feller SE, Pastor RW, Bax A (1995) Rotational diffusion anisotropy of human ubiquitin from ^{15}N NMR relaxation. J Am Chem Soc 117:12562–12566

Woessner DE (1962) Nuclear spin relaxation in ellipsoids undergoing rotational Brownian motion. J Chem Phys 40:647–654

Yamakawa H (1971) Modern theory of polymer solutions. Harper & Row, New York